Journal of Anatomy

J. Anat. (2013) **222**, pp193–202 doi: 10.1111/joa.12004

The cast imaging of the osteon lacunar-canalicular system and the implications with functional models of intracanalicular flow

Ugo E. Pazzaglia[1] and Terenzio Congiu[2]

[1]*Department of Specialità Chirurgiche, Scienze Radiologiche, Mediche e Sanità Pubblica, Orthopaedic Clinic of the University of Brescia, Brescia, Italy*
[2]*Department of Scienze Chirurgiche e Morfologiche, University of Insubria, Varese, Italy*

Abstract

A casting technique with methyl-methacrylate (MMA) was applied to the study of the osteon lacunar-canalicular network of human and rabbit cortical bone. The MMA monomer infiltration inside the vascular canals and from these into the lacunar-canalicular system was driven by capillarity, helped by evaporation and the resulting negative pressure in a system of small pipes. There was uniform, centrifugal penetration of the resin inside some osteons, but this was limited to a depth of four to five layers of lacunae. Moreover, not all of the osteon population was infiltrated. This failure can be the result of one of two factors: the incomplete removal of organic debris from the canal and canalicular systems, and lack of drainage at the osteon external border. These data suggest that each secondary osteon is a closed system with a peripheral barrier (represented by the reversal line). As the resin advances into the osteon, the air contained inside the canalicula is compressed and its pressure increases until infiltration is stopped. The casts gave a reliable visualization of the lacunar shape, position and connections between the lacunae without the need for manipulations such as cutting or sawing. Two systems of canalicula could be distinguished, the equatorial, which connected the lacunae (therefore the osteocytes) lying on the same concentric level, and the radial, which established connections between different levels. The equatorial canalicula radiated from the lacunar border forming ramifications on a planar surface around the lacuna, whereas the radial canalicula had a predominantly straight direction perpendicular to the equatorial plane. The mean length of the radial canalicula was 40.12 ± 10.26 μm in rabbits and 38.4 ± 7.35 μm in human osteons; their mean diameter was 174.4 ± 71.12 nm and 195.7 ± 79.58 nm, respectively. The mean equatorial canalicula diameter was 237 ± 66.04 nm in rabbit and 249.7 ± 73.78 nm in human bones, both significantly larger ($P < 0.001$) than the radial. There were no significant differences between the two species. The lacunar surface measured on the equatorial plane was higher in rabbit than in man, but the difference was not statistically significant. The cast of the lacunar-canalicular network obtained with the reported technique allows a direct, 3-D representation of the system architecture and illustrates how the connections between osteocytes are organized. The comparison with models derived by the assumption of the role of hydraulic conductance and other mechanistic functions provides descriptive, morphological data to the ongoing discussion on the Haversian system biology.

Key words: interstitial fluid flow; lacunar-canalicular system; osteocyte; osteon.

Introduction

Several methods have been applied to the study of the osteocyte lacunar-canalicular system using different imaging techniques (Ejiri & Ozawa, 1982; Kamioka et al., 2001; Hirose et al., 2007). However, various experimental limitations allowed for the assessment of only isolated or incompletely interconnected osteocytes. Three-dimensional reconstructions of the osteocyte morphological structure have been obtained with confocal laser scanning micros-

Correspondence
Ugo E. Pazzaglia, Department of Specialità Chirurgiche, Scienze Radiologiche, Mediche e Sanità Pubblica, Orthopaedic Clinic of the University of Brescia, Brescia, Italy. T: 0039 030 393832; F: 0039 030 397365; E: ugo.pazzaglia@spedalicivili.brescia.it

Accepted for publication *26 September 2012*
Article published online *22 October 2012*

copy (Sugawara et al., 2005) but only on the limited thickness of the chick calvaria or with serial FIB/SEM imaging (Schneider et al., 2011) in the mouse femur, where a true system of secondary osteons is not present.

Resin-cast imaging of the lacunar-canalicular system has been obtained in hound mandibles (Lu et al., 2007; Kubek et al., 2010) or at the bone-bioactive glass interface (Gorustovich, 2010), but in all these studies the imaging was limited to a planar representation of a transverse section of the osteon or to the plane surface of the neoformed bone around bioglass particles.

Application of casting techniques to the study of the osteon lacunar-canalicular system is difficult because of the small size of the canalicula, which hampers the penetration of the resin, as well as technical problems in the cleaning, desiccation and etching of the bone specimens.

We present a casting technique that was applied to human and rabbit cortical bone with the aim of illustrating the 3-D organization of the osteon lacunar-canalicular system. The decision to use specimens from two different species (man and rabbit) was due to earlier observations that the canal network intersections, the size of the osteons, the osteocyte interconnections and consequently the complexity of the lacunar-canalicular system might be lower in rabbit than in man (Pazzaglia et al., 2008). We supposed that the lacunar-canalicular system analysis in the rabbit would therefore be less difficult because of the less crowded vascular canal casts. However, the limited penetration of the resin within the canalicular system of both species osteons reduced any benefit.

Both the experimental observations related to the technique and the reproducible artifacts contributed to a 3-D description of the canalicular network architecture. It was compared with the theoretical models based on hydraulic conductance and fluid flow within the canalicular system (Mishra & Knothe Tate, 2003).

This study will enhance knowledge of the normal 3-D organization and function of the Haversian lacunar-canalicular system, expanding the anatomical basis for comparison with aging and metabolic bone diseases.

Materials and methods

Human cortical bone specimens of femur and tibia were obtained from the subjects of an earlier research including three male, healthy young males (Pazzaglia et al., 2012c). This study was approved by the Ethic Committee of 'Spedali Civili di Brescia' and by the Council of the Department of 'Specialità Chirurgiche, Scienze Radiologiche e Medico-forensi' of Brescia University. The specimens consisted of parallelepipeds of cortical bone 10 × 6 × 6 mm, which included the periosteal and the endosteal surface. The specimens could be easily oriented because the 10-mm height corresponded to the longitudinal axis of the diaphysis. They had been stored in buffered formaldehyde 4% until processed.

The rabbit bones used were specimens left over from a previous experiment (Pazzaglia et al., 2008), consisting of a five segments of the femur diaphysis, about 10 mm long, stored in buffered formaldehyde 4% until processed. The rabbits were White New Zealand, each about 3.5 kg, 8 months of age and not submitted to any treatment.

All the specimens were cleaned from soft tissues in a 40% solution of hydrogen peroxide for 30 days and dehydrated in an ascending scale of ethanol; each step in the dehydration scale (70, 80, 95, 100 and 100%) was followed by ultrasonication for 30 min. They were finally critical-point dried with CO_2 (Emitech K850, Emitech Ltd, Ashford, Kent, UK) at 35–40 °C and 80 bar of pressure.

Liquid methyl-methacrylate resin after neutralization of hydroquinone with N,N-dimethyl-*p*-toluidine (1%), was mixed with benzoyl peroxide (0.1 mg 1 mL^{-1} of methyl-methacrylate) in a Petri dish forming a layer of 3 mm of the fluid. Both the monomer and the experimental set were kept at 7 °C. The dehydrated, un-decalcified specimens were then put on the flat bottom of the Petri dish and oriented in such a way that the longitudinal axis of each specimen was perpendicular to the bottom of the dish, with the level of the resin reaching to about one-third of the height of the specimens. Penetration of the resin occurred by capillarity inside the vascular canals and the lacunar-canalicular system. After methyl-methacrylate polymerization, the blocks with the base of resin were removed from the Petri dish and the upper surface of the specimens ground on sand paper (granularity 1000). The etching process to remove the bone was carried out by immersing the blocks alternatively in 15% HCl solution (pH 0.79) to decalcify the matrix and in 15% KOH solution (pH 13.82) to digest the organic fraction of the matrix (Fig. 1); these passages were repeated several times over a period of 60 days.

When the resin casts were sufficiently free of bone matrix, they were again dehydrated in the ascending scale of ethanol, dried in hexamethyldisilazane and coated with a thin layer of gold-

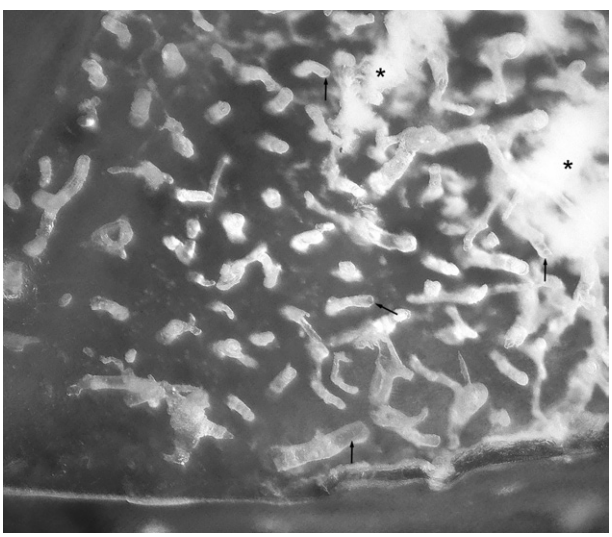

Fig. 1 Image of the cast during the processing phase of bone matrix decalcification/maceration. Casts of the Haversian canals cleared from the surrounding matrix come out perpendicularly from the MMA base. Some of them are hollow (arrows) as a result of the slowed polymerization of the resin. The white material between canal casts (asterisks) is as yet undigested bone matrix.

palladium with a sputter Emitech 550. Observation was carried out with a scanning electron microscope Philips XL30.

Morphometry

The surface of the osteonal central canal was chosen as the reference frame for the analysis of the osteocyte lacunar-canalicular system (Fig. 2). Different levels of resin penetration from the central canal into the lacunar-canalicular network were obtained: first, those where the resin infiltration was limited to the vascular canal and to the first segment of the canalicula which flowed into the canal lumen, and secondly, those where the resin seeped deeper into the lacunar-canalicular system of the osteon, allowing the lacunae lying on different levels and the frame of interconnecting dendrites to be shown. In the second group it was possible to distinguish casts including only the first lacunar layer (mono-layer) and those displaying several layers (multi-layer).

The morphometric evaluation was carried out on selected fields and segments of the central canal casts because the resin penetration was not uniform along the single canal in either human or rabbit bones. The density of lacunar casts for the first layer was assessed in mono-layered segments of the central canal by measuring the hemi-canal segment surface (π r. h) and counting the number of lacunar casts on this surface. It was assumed that the transverse section of the canal was a regular circumference (Fig. 2A,B).

The planar area of the lacunar cast bone face, the number of equatorial and radial dendrites (Fig. 3), and the geometrical pattern of the lacunar systems were determined in both the mono-layered and multi-layered casts. The equatorial canaliculi arose from the cone of emergence in the lacunar cast wall.

An estimate of the radial canalicula length, and of the equatorial and radial canalicula diameters was carried out at a higher enlargement, selecting those casts where it was possible to follow the whole canalicular course connecting neighbouring lacunae. The mean diameter of equatorial canalicula was measured at the mid-point between bifurcations, and that of the radial at regular intervals of 20 μm.

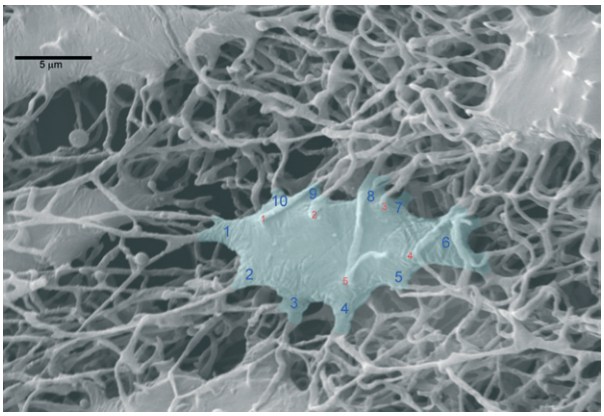

Fig. 3 Osteocyte lacunar cast from a mono-layer infiltration depth of the lacunar-canalicular network. The light-blue tinted area corresponds to the measured, lacunar bone surface: it includes the spur cones of the equatorial processes: they are numbered in blue and the radial in red.

Eight independent samples (three from human bone and five from rabbits) were analyzed. There were mono-layer casts properly infiltrated by the resin for mean lacunar cast density assessment in human bone and none in rabbit femurs. The other parameters (lacunar surface area, equatorial and radial canalicula number, equatorial and radial canalicula diameter, and radial canalicula length) were measured in selected fields where the electron beam was as far as possible perpendicular to the examined surface.

The measurements were carried out with the program CELL (Soft Imaging System GmbH, Munster, Germany) and each parameter was compared with Student's *t*-test between specimens of human and rabbit bone.

Results

The resin inside the vascular canal formed a concentric layer on the inner wall (Fig. 1) in both rabbit and human bone. From the inside it infiltrated the osteocyte lacunae and the canalicular network (Fig. 3). The depth of penetration into the lacunar-canalicular network allowed the characterization of three types of casts:

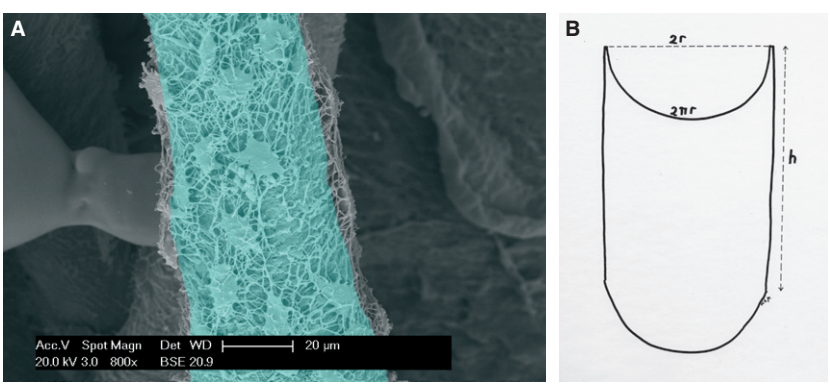

Fig. 2 (A) Vascular canal cast from a mono-layer infiltration depth of the lacunar-canalicular network. The light-blue tinted area corresponds to a segment of the hemi-canal surface used to estimate the density of the lacunar cast first layer (n mm^{-2}). (B) Diagram illustrating the method of assessment of the hemi-canal segment surface (nr.h). It was assumed that the transverse section of the canal was a regular circumference.

(i) Bare vascular canals, where the cast reproduced the collagen fibrils pattern of the inner surface of the central canal. The fibril bundles showed an ordered parallel disposition with different angles to the canal axis (Fig. 4A); they converged in an orderly way in correspondence with canal ramifications. The canalicular openings of the first layer of osteocyte lacunae could be distinguished between the collagen bundles as short processes sticking out from the canal surface. Their distribution did not look uniform and they appeared denser in delimited zones of circular or oval shape (Fig. 4B). No structural differences were observed between rabbit and human bone.

(ii) Mono-layer of osteocyte lacunar casts, with flattened and roundish imprints of the cells. Equatorial dendrites emerging from the perimeter formed a reticular network which connected all the lacunae casts lying on the same plane. From the bone surface (that facing the periphery of the osteon) emerged short processes with rounded top ends, which indicated the arrest of the resin penetration within the centrifugal radial canalicula. In this type of cast (obtained only in human specimens) it was possible to measure the hemi-surface of the central canal, and the number of osteocyte lacunae and consequently their density (Fig. 2A,B). The area of the lacuna and the number of equatorial dendrites was determined by tracing the equatorial perimeter as described in Materials and methods (Fig. 3). There were no significant differences when the mean values of lacunar surface area, equatorial and radial canalicular number (the latter limited to the hemi-surface) were compared between rabbit and human bone specimens (Table 1).

(iii) Multi-layer osteocyte lacunar casts revealed a denser and more complex network because of the lacunar layers overlapping and the interconnections between osteocyte lacunae, which mixed equatorial and radial processes (Fig. 5). The radial processes consisted of a bundle of straight and basically parallel filaments with no or very few ramifications and fusions (Fig. 6). The dendrite density limited the possibility for observing the whole thickness of the resin-injected sector of the osteonal canalicular system. However, at least one underlying layer of lacunar casts could be recognized through the network of dendrites. The radial canalicular casts appeared stretched along the central canal axis (Fig. 6) as an effect of shrinkage of the injected part of the osteonal cast (longitudinal shrinkage). The MMA scaffold, however, withstood this deformation very well, as no fractures of the thin filaments corresponding to the canalicula were observed.

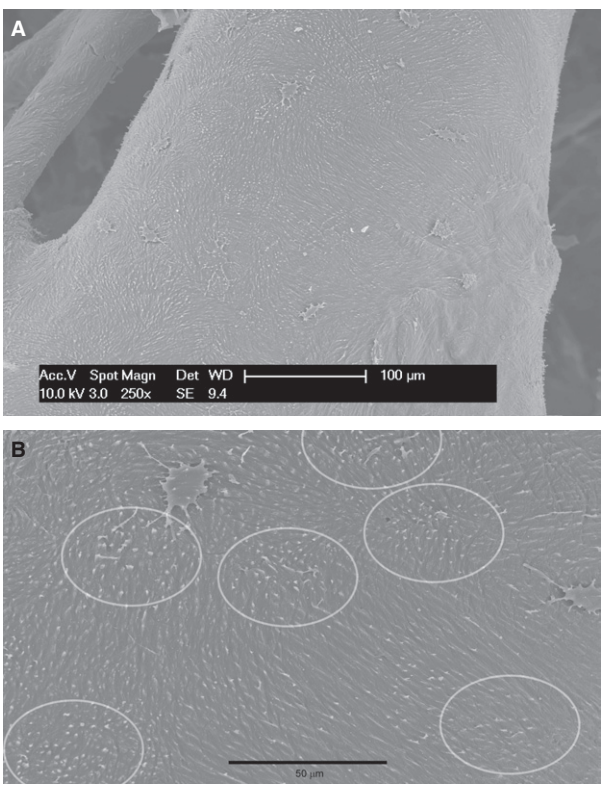

Fig. 4 (A) Cast of a bare vascular canal where the resin penetrated inside the first tract of the canalicula openings into the canal lumen. The collagen fibril pattern is reproduced by the cast showing the ordered, parallel disposition with different angles with the canal axis. Scattered lacunae have been infiltrated by the progression of the resin within the lacunar-canalicular system. (B) Detail of (A) showing the initial cast of the canalicula connecting the canal lumen with the intraosteonal system. The oval areas where they are more densely packed correspond to the positions of the osteocyte not yet infiltrated by the resin.

The concept of longitudinal shrinkage was confirmed in the human specimens by the comparison of lacunar triangulation between mono-layer and the most superficial network of the multi-layered casts (Fig. 7A,B); in the latter, the triangular meshes were observed to be more stretched along the axis of the vascular canal. The triangulation was carried out by tracing the shorter segment between triplets of osteocyte lacunar casts. The choice of the triplets was determined by the density of connections in such a way that the triangulation resulted in the more accurate description of the equatorial canalicula distribution in the mono-layer casts, whereas in the multi-layered casts the pattern was also conditioned by the radial canalicula.

Radial, single canalicula could be identified and followed at higher magnification from one lacunar cast to the next, either lying on the same plane or placed on sequential parallel planes (Fig. 8A,B). The mean diameter was measured as reported in Material and methods. Equatorial canalicula could be measured only in mono-layer osteocyte lacunar

Table 1 Morphometry of the lacunar-canalicular system in rabbit and human cortical bone.

	Mean lacunar cast density (1st layer)		Mean lacunar surface area		Mean equatorial canalicular number	Mean Radial canalicular number		Mean radial canalicular		Mean equatorial canalicular
	n	(n mm^{-2})	*n*	(μm^2)	for lacuna (*n*)	for lacuna (*n*)	*n*	length (μm)	*n*	diameter (nm)
Rabbit cortical bone	–	–	22	110.3 ± 21.67	8.09 ± 1.55	8.7 ± 1.6	8	40.12 ± 10.26	30	174.4 ± 71.1*	237 ± 66.04*
Human cortical bone	12	3215 ± 548.7	12	105.9 ± 23.34	7.5 ± 1.75	8.8 ± 1.75	20	38.4 ± 7.36	50	195.7 ± 79.5**	249.7 ± 73.78**

*$P \leq 0.001$; **$P \leq 0.001$.

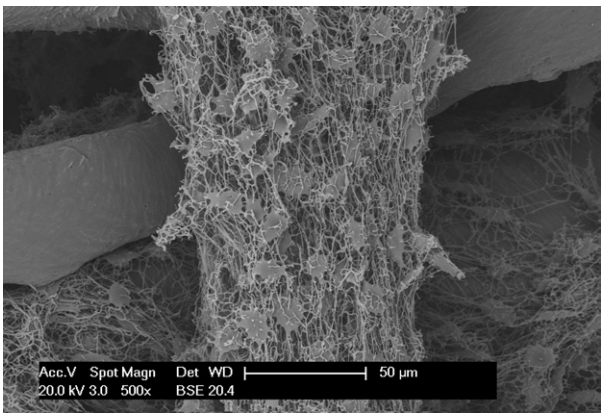

Fig. 5 Multi-layered cast: the canalicular network is formed by a mixture of equatorial and radial processes. Longitudinal shrinkage has stretched the radial canalicula along the axis of the central canal. Between the meshes can be observed the lacunar casts of the underlying layer.

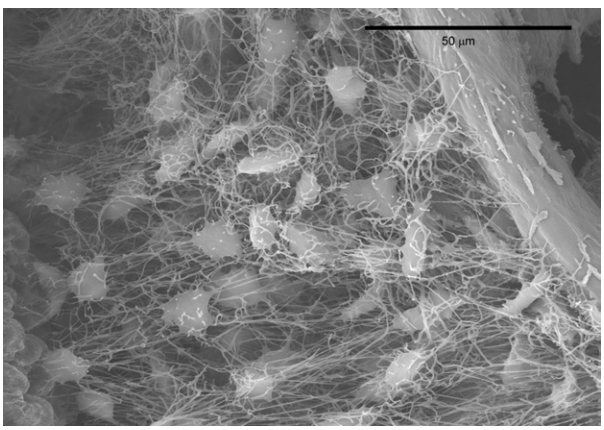

Fig. 6 Detail of multi-layered cast: the canalicular network is formed by a mixture of equatorial and radial processes. The latter have been stretched by longitudinal shrinkage.

casts, but the radial canalicula could be measured in multi-layer casts. The differences examined between equatorial and radial canalicula were length, cone of emergence, ramifications, and the mean diameter (Table 1), and the results showed larger equatorial canaliculi ($P < 0.001$).

The mean lacunar density of mono-layer casts in human bone was 3215 ± 548.7 n mm^{-2}; it was not measurable in rabbit bone specimens because there were no mono-layer casts in this group. No significant differences were observed between the other parameters pertaining to lacunae and canalicula of human and rabbit bones (Table 1).

Discussion

Visualization and appreciation of the three-dimensional organization of the osteocyte lacunar system and of the canalicular network in cortical compact bone is difficult to

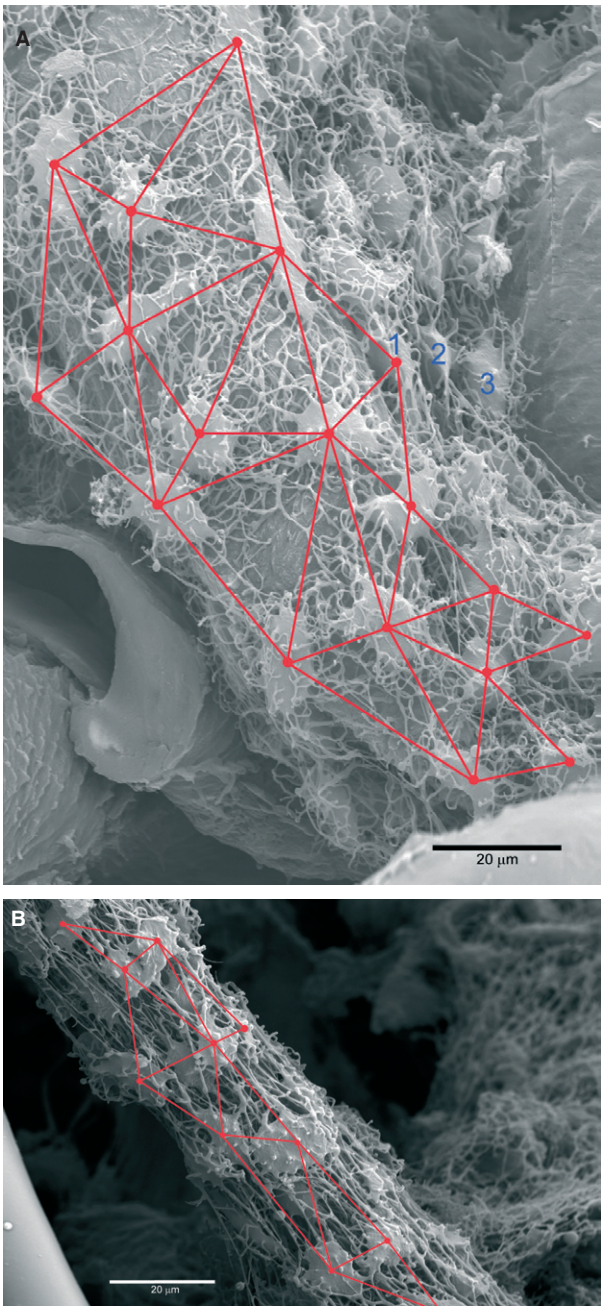

Fig. 7 (A) Triangulation of the lacunar network of the mono-layer cast. (B) Triangulation of the lacunar network of multi-layer cast. The triangular meshes are stretched along the central canal axis (longitudinal shrinkage) because the lacunar-canalicular system was not supported and stiffened by the bone matrix scaffold after the decalcification/maceration process.

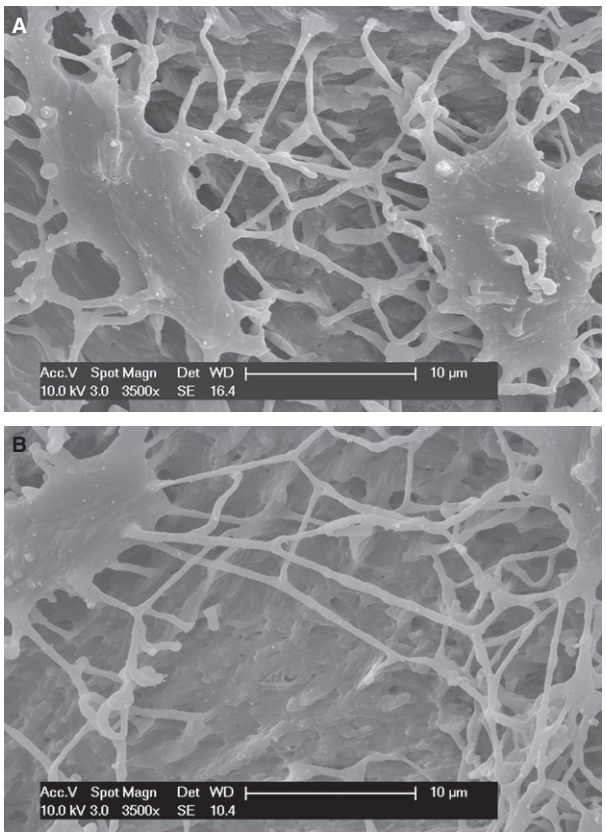

Fig. 8 (A) Equatorial canalicula cast network: the canicula are formed by processes emerging from a cone, with many ramifications which form a network. (B) Radial canalicula casts are formed by elongated and straight processes with no, or very few, ramifications; their origin is from the convex bone or vascular surface of the lacunar cast or from equatorial ramifications.

study because of the small size of the system and the fact that it is embedded within a densely mineralized matrix.

Different imaging techniques employing light microscopy, SEM, confocal SEM or serial FIB/SEM imaging have been used to produce three-dimensional reconstructions of this system (Ham, 1952; Ejiri & Ozawa, 1982; Kamioka et al., 2001; Sugawara et al., 2005; Hirose et al., 2007; Schneider et al., 2011; Pazzaglia et al., 2012a). Casting techniques after infiltration of bone with methyl-methacrylate and etching of the mineralized bone matrix have been used to obtain a visualization of the osteocyte lacunae and the system of canalicula (Marotti et al., 1985; Okada et al., 2002; Feng et al., 2006; Lu et al., 2007; Gorustovich, 2010; Kubek et al., 2010). However, the lacunar and canalicular spaces evidenced were limited to single or thin layers of a cortical section.

The casting technique we employed is new because the advancement of the MMA monomer inside the vascular canals and from these into the lacunar-canalicular system of the corresponding osteon proceeded by capillarity from the bottom to the top of the specimen. The force driving the progression of the liquid monomer is capillarity, helped by evaporation and the resultant negative pressure it can exert when applied to a system of small pipes. The mechanism is the same as that occurring in nature to regulate the circulation of fluids in plants (Tyree & Ewers, 1991; Yang & Tyree,

1994; Ennos, 1999). Several factors control the driving force, e.g. the superficial tension, which is lower in MMA than in H_2O, and the volatility (evaporation), which conversely is much higher in MMA. By acting on these factors it is possible to optimize the resin infiltration: for example, in this study it was not carried out under vacuum as reported by Kubek et al. (2010) and the temperature of the experimental environment was kept at 7 °C to slow down evaporation. The resin infiltration proceeded centrifugally from the central canal toward the periphery of the osteon with a very good infilling of the canalicula, whereas the specimen external surface was not covered by resin, which made possible the attack of the etching agents on the mineralized matrix.

A further, necessary condition for a satisfactory impregnation is the complete removal of soft tissues from inside the lacunae and the canalicular network, which we obtained with a prolonged soaking of the specimens in a concentrated solution of hydrogen peroxide, with dehydration/delipidization in acetone and repeated ultrasonications.

The mechanism of centrifugal infiltration of the osteon from the central canal was confirmed by observing the specimen while rotating and tilting it in all directions. We could control with a very high degree of approximation the depth of resin penetration inside the lacunar-canalicular system, determining the formation of bare vascular canals, mono-layer and multi-layered osteocyte lacunar casts. These casts allowed us to explore the inner organization of the network without manipulations such as cutting or sawing, which would have damaged its structure. The network of canalicula was very delicate, with diameters varying from 73 to 480 nm, but in no point of the cast were interruptions or fractures of the meshes observed. The radial canalicula emerging from the lacunar bone face of the most superficial layer of lacunae, ended with a rounded cap, which suggested an arrest of the resin progression rather than a traumatic fracture.

The cast gave a reliable visualization of the lacunar shape and position and of the connections between the cells. Two systems of canalicula could be distinguished, the equatorial evidenced by the mono-layer casts, which connected the lacunae (therefore the osteocytes) lying on the same concentric level, and the radial, which established connections between different levels. The radial systems were documented in multi-layered osteocyte lacunar casts as a bundle of straight and basically parallel canalicular casts with no or few ramifications and anastomoses. However, the two systems were not completely independent because radial canalicula originating from equatorial ramifications were also observed.

There was an evident discrepancy between the image of these casts and the structural pattern obtained by osteon sectioning and reconstruction (Pazzaglia et al., 2012a). This discrepancy is due to an artifact produced by collapse of the canalicular network when the mineralized collagen matrix

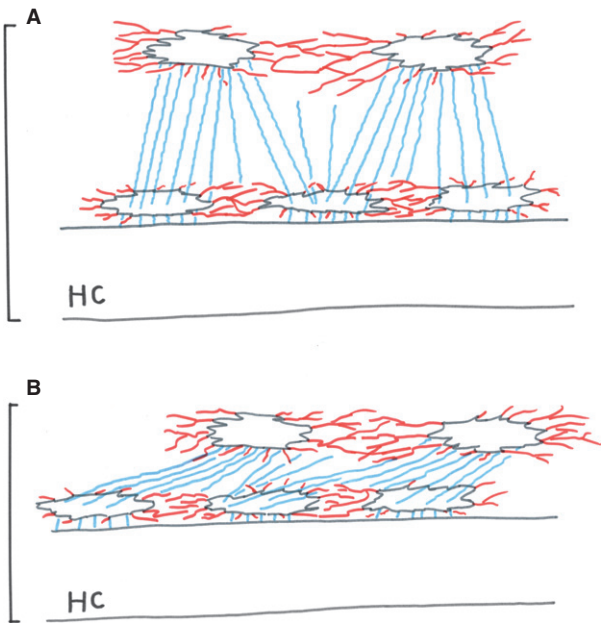

Fig. 9 Scheme of the equatorial canalicular network (red) in mono-layer casts (A) and the complex pattern established by equatorial and radial (blue) canalicular network in multi-layer casts (B) deformed by longitudinal shrinkage.

was removed by maceration (longitudinal shrinkage). However, because of the MMA elasticity, there were no fractures of the canalicular network, which appeared stretched and flattened along the central canal (Fig. 9). This artifact in multi-layered casts evidenced the canalicular radial systems and masked the equatorial, allowing length and diameter measurements of the former.

The size of the canalicular diameter has been reported variously as 150–350 nm (You et al., 2004), 700–100 nm (Marotti et al., 1979; Marotti, 1990, 1996), 85–100 nm (Cooper et al., 1966), and 150–200 nm (Palumbo et al., 1990a,b; Steflik et al., 1994). However, these measurements were carried out with TEM on transverse sections of the canalicula or on short longitudinal segments. The cast reproduction of the canalicular system allowed the separation of single canalicula extending from one osteocytic lacuna to the neighbouring lacuna and the measurement of the length, which is not accessible with techniques based on sectioning such as TEM. The diameters were measured from the outside at regular intervals and for the whole length. The mean length of radial canalicula assessed on casts was 38.45 ± 7.35 μm in human specimens, with a good correspondence with measurements carried out with light microscopy in undecalcified, transverse sections of the osteon (Pazzaglia et al., 2012a). The mean diameter was 195.7 ± 79.58 nm, within the range of previous determinations carried out with TEM. Enlargements or swellings along their course could be observed, which would be compatible with an inter-dendritic connection through gap-junction

when the processes of the two connecting cells may have overlapped for a certain tract.

The osteon lacunar-canalicular system evidenced by this cast technique was observed to be structured with radial connections between osteocyte lacunae and the central canal and with the equatorial network, which establishes a communication among lacunae lying approximately on the same concentric layer. This could suggest a link with the osteonal lamellar structure, but no evidence can be obtained on this point by the casting technique because the whole collagenic matrix was removed by maceration. The model of this organization (Fig. 10) corresponds to the pattern of osteon infilling and osteocyte radial domain presented in a previous paper (Pazzaglia et al., 2012a). The active osteoblast morphology is characterized by a bundle of processes emerging from the secretory surface of the cells as they move along radial trajectories toward the central canal (Pritchard, 1956; Ham, 1957; Schenk & Willenegger, 1967; Palumbo et al., 1990a; Pazzaglia et al., 2010, 2012b), whereas the equatorial system is formed when the synthetic activity of the osteoblasts slows down and the cells flatten, modulating their shape into that of the osteocytes (Marotti, 1990; Palumbo et al., 1990b).

We compared our model of the osteon lacunar-canalicular system with that proposed by Mishra & Knothe Tate (2003) because the architecture of the canalicular network they deduced from theoretical assumptions looked very similar to that derived from the osteon casts: in fact, their pattern reproduced rhomboidal meshes, but they did not consider the coplanar connections established between osteocyte lacunae by the equatorial canalicula, which would transform the network pattern into one based on triangular meshes. In this model, the authors assumed that the architecture of the osteonal canalicular system was defined by the pericellular fluid space to optimize the transport of fluids and solutes between the blood supply and bone cells. Their analysis assigned to the hydraulic conductance a critical role in determining the structural organization of the canalicular system. The basic assumptions consisted in:

(i) a flow of the pericellular fluid within the canalicular system;
(ii) the flow direction from the Haversian canal to the periphery of the osteon;
(iii) the increment of the canalicula sectional area (through the rise of their number) with the increasing distance from the blood supply.

Well established anatomical data disagree with these assumptions because the formation of the secondary osteons always proceeds from the reversal line toward the central canal in the opposite direction (centripetal) to that of the hypothesized fluid flow and consequently the canalicular system in its development is convergent rather than divergent.

A further observation is that interconnections between the osteocyte lacunae are limited to the environment of the secondary osteon, whereas connections between neighbouring osteons are practically non-existent and the reversal line (or the reversal cylinder in 3D) represents a barrier between individual osteonal systems.

Hydrostatic permeability of the osteon has been tested by Guoping et al. (1987); they documented a fluid flow through the cortex from the endosteal to the periosteal surface driven by high pressure. However, their model shows the flow through the Haversian and the Volkmann' canals, and not in the canalicular system.

The mechanism of an intracanalicular flow necessarily requires a liquid drain, which in the model suggested by Piekarski & Munro (1977) and later theorized on a mathematical basis by Petrov & Pollack (2003) was assigned to inversion of the flow direction induced by the cyclic load, not dissimilar to that inside the articular cartilage.

The casting technique we applied to the cortical bone lacunar-canalicular system supported the hypothesis of a very low permeability of the outer osteon surface (corresponding to the reversal line), as even the air inside the canalicula could not escape under the pressure of the infiltrating MMA. These observations together with the rigid osteonal, lamellar scaffold, in this respect very different from the joint cartilage, give rise to doubts about

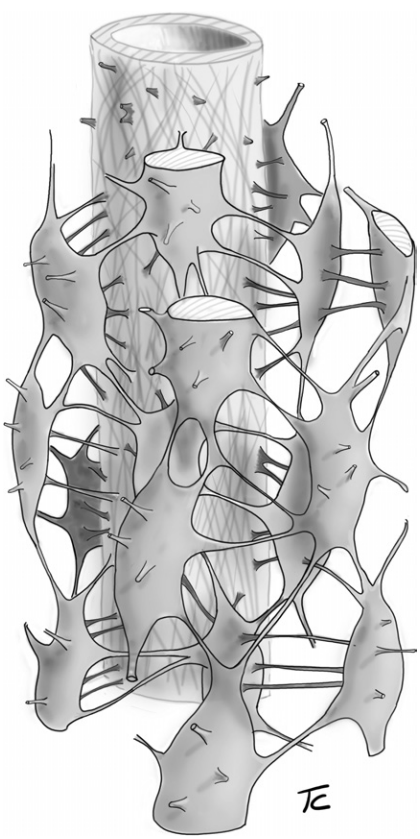

Fig. 10 3-D scheme of the lacunar-canalicular system organization.

assumptions of a flow or stream along the spaces of the lacunar-canalicular system. The architecture of the cast model is consistent with the hypothesis of a rather static bone pericellular fluid or, in any case, of a very slow rate of exchange with the perivascular fluid of the central canal. Ions, oxygen and metabolites are small soluble molecules, therefore once they are added to a volume of fluid they balance into the whole fluid volume without flow or stream of liquid.

That the osteocyte/dendrite network surface is wet by interstitial fluid is an ascertained fact and membrane transport mechanisms can convey metabolites into the cells (Shapiro, 1988; Kusuzaki et al., 2000). Connections between bone cells through gap junctions were documented with transmission electron microscopy and atomic force microscopy (Weiniger & Holtrop, 1974; Pawlicki, 1975; Stanka, 1975; Doty, 1981; Larsen, 1983). The osteocyte processes stay in the centre of the canalicula, with a gap between the cellular membrane and the canalicular wall (You et al., 2004): this suggests that extracellular fluid can pass through the system in an intracanalicular but extracellular/extra-processes position (Doty, 1981; Shapiro, 1988). Conversely, these gaps have also been interpreted as artifacts due to shrinkage of the cell protoplasm, which would imply that metabolite transport occurs within the cell membrane (Weiniger & Holtrop, 1974). The question is still unanswered and no definitive evidence has been produced so far in favour of the first or the second hypothesis; however, in both cases, the bone intracanalicular fluid flow is not a necessary condition for the nutrition of the cells.

The casting technique of the osteonal canalicular systems we presented, even if limited to the inner layers and with some artifacts produced by the MMA plasticity, gave a direct, 3-D description of the system in normal bone. Future studies can improve the quality and the accuracy of the scaffold reproduction and extend the observations to variations induced by age and bone diseases.

Acknowledgements

The study was carried out with a scanning electron microscope of 'Centro Grandi Strumenti' University of Insubria and was supported by research funds of Brescia University, Department of 'Specialità Chirurgiche, Scienze Radiologiche, Mediche e Sanità Pubblica'.

References

Cooper RR, Milgram JW, Robinson RA (1966) Morphology of the osteon. An electron microscopy study. *J Bone Joint Surg* **48A**, 1239–1271.

Doty SB (1981) Morphological evidence of gap junctions between bone cells. *Calcif Tissue Int* **33**, 509–512.

Ejiri S, Ozawa H (1982) Scanning electron microscopic observations of rat tibia using HCl-collagenase method. *Arch Histol Jap* **45**, 399–404.

Ennos AR (1999) The aerodynamics and hydrodynamics of plants. *J Exp Biol* **202**, 3281–3284.

Feng JQ, Ward LM, Liu S, et al. (2006) Loss of DMP1 causes rickets and osteomalacia and identifies a role for osteocytes in mineral metabolism. *Nat Genet* **38**, 1310–1315.

Gorustovich AA (2010) Imaging resin-cast osteocyte lacuna-canalicular system at bone-bioactive glass interface by scanning electron microscopy. *Microsc Microanal* **16**, 132–136.

Guoping L, Bronk JT, An K-N, et al. (1987) Permeability of the cortical bone of canine tibias. *Microvasc Res* **34**, 302–310.

Ham AW (1952) Some histophysiological problems peculiar to calcified tissues. *J Bone Joint Surg* **34A**, 701–728.

Ham AW (1957) *Histology*. pp. 271–338. Philadelphia: JB Lippincott Co.

Hirose S, Li M, Kojima T, et al. (2007) A histological assessment of the distribution of the osteocytic lacunar canalicular system using silver staining. *J Bone Miner Metab* **25**, 374–382.

Kamioka H, Honjo T, Takano-Yamamoto T (2001) A three-dimensional distribution of osteocyte processes revealed by the combination of confocal laser scanning microscopy and differential interference contrast microscopy. *Bone* **28**, 145–149.

Kubek DJ, Gattone VH, Allen MR (2010) Methodological assessment of acid-etching for visualizing the osteocyte lacunar-canalicular network using scanning electron microscopy. *Microsc Res Tech* **73**, 182–186.

Kusuzaki K, Kageyama N, Shinjo H, et al. (2000) Development of bone canaliculi during bone repair. *Bone* **27**, 655–659.

Larsen WJ (1983) Biological implications of gap junction structure, distribution and composition: a review. *Tissue Cell* **15**, 645–671.

Lu Y, Xie Y, Zhang S, et al. (2007) DMP1-targeted Cre expression in odontoblasts and osteocytes. *J Dent Res* **86**, 320–325.

Marotti G (1990) *Ultrastructure of Skeletal Tissue*. Boston: Kluwer Academic Publisher.

Marotti G (1996) The structure of bone tissues and the cellular control of their deposition. *Ital J Anat Embryol* **101**, 25–79.

Marotti G, Delrio N, Marotti F, et al. (1979) Quantitative analysis of the bone destroying activity of osteocytes and osteoclasts in experimental disuse osteoporosis. *Ital J Orthop Traumatol* **5**, 255–240.

Marotti G, Remaggi F, Zaffe D (1985) Quantitative investigation on osteocyte canaliculi in human compact and spongy bone. *Bone* **6**, 335–337.

Mishra S, Knothe Tate ML (2003) Effect of lacunar-canalicular architecture on hydraulic conductance in bone tissue: implications for bone health and evolution. *Anat Rec* **273A**, 752–762.

Okada S, Yoshida S, Ashrafi SH, et al. (2002) The canalicular structure of compact bone in the rat at different ages. *Microsc Microanal* **8**, 104–115.

Palumbo C, Palazzini S, Marotti G (1990a) Morphological study of intercellular junctions during osteocyte differentiation. *Bone* **11**, 401–406.

Palumbo C, Palazzini S, Zaffe D, et al. (1990b) Osteocyte differentiation in the tibia of newborn rabbit: an ultrastructural study of the formation of cytoplasmic processes. *Acta Anat* **137**, 350–358.

Pawlicki R (1975) Bone canaliculus endings in the area of the osteocyte lacuna. Electron-microscopic studies. *Acta Anat* **91**, 292–304.

Pazzaglia UE, Bonaspetti G, Ranchetti F, et al. (2008) A model of the intracortical vascular system of long bones and its orga-

nization: an experimental study in rabbit femur and tibia. *J Anat* **213**, 183–193.

Pazzaglia UE, Congiu T, Marchese M, et al. (2010) The shape modulation of osteoblast-osteocyte transformation and its correlation with the fibrillar organization in secondary osteons. A SEM study employing the graded osmic maceration technique. *Cell Tissue Res* **340**, 533–540.

Pazzaglia UE, Congiu T, Franzetti E, et al. (2012a) A model of osteoblast-osteocyte kinetics in the development of secondary osteons in rabbits. *J Anat* **220**, 372–383.

Pazzaglia UE, Congiu T, Zarattini G, et al. (2012b) The canalicular system and the osteoblast domain in human secondary osteons. *Anat Histol Embryol*, doi:10.1111/j.1439-0264.20120115x.

Pazzaglia UE, Congiu T, Marchese M, et al. (2012c) SEM morphometry and patterns of Haversian lamellar bone. A study in the human tibia employing Na_3PO_4 etching and polarized light microscopy. *Anat Rec* **295**, 1421–1429.

Petrov N, Pollack SR (2003) Comparative analysis of diffusive and stress induced nutrient transport efficiency in the lacunar-canalicular system of osteons. *Biorheology* **40**, 347–353.

Piekarski K, Munro M (1977) Transport mechanism operating between blood supply and osteocytes in long bones. *Nature* **269**, 80–82.

Pritchard JJ (1956) General anatomy and histology of bone. In: *The Biochemistry and Physiology of Bone*. (ed. Bourne GH), pp. 1–26. New York: Academy Press.

Schenk R, Willenegger H (1967) Morphological findings in primary fracture healing. *Symp Biol Hungaricae* **7**, 75–86.

Schneider P, Meier M, Wepf R, et al. (2011) Serial FIB/SEM for quantitative 3D assessment of the osteocyte lacuna-canalicular network. *Bone* **49**, 304–311.

Shapiro F (1988) Cortical bone repair. The relationship of the lacunar-canalicular system and intercellular gap junction to the repair process. *J Bone Joint Surg* **70A**, 1067–1081.

Stanka P (1975) Occurrence of cell junctions and microfilaments in osteoblasts. *Cell Tissue Res* **159**, 413–422.

Steflik DE, Sisk AL, Parr GR, et al. (1994) Transmission electron and high-voltage electron microscopy of osteocyte cellular processes extending to the dental implant surface. *J Biomed Mater Res* **28**, 1095–1107.

Sugawara Y, Kamioka H, Honjo T, et al. (2005) Three-dimensional reconstruction of chick calvarian osteocytes and their cell processes using confocal microscopy. *Bone* **36**, 877–883.

Tyree MT, Ewers FW (1991) The hydraulic architecture of trees and other woody plants. *New Phytol* **119**, 345–360.

Weiniger JM, Holtrop ME (1974) An ultrastructural study of bone cells: the occurrence of microtubules, filaments and tight junctions. *Calcif Tissue Res* **14**, 15–19.

Yang S, Tyree MT (1994) Hydraulic architecture of *Acer saccharin* and *A. rubrum*: comparison of branches to the whole trees and the contribution of leaves to hydraulic resistance. *J Exp Bot* **45**, 179–186.

You L-D, Weinbaum S, Cowin SC, et al. (2004) Ultrastructure of the osteocyte process and its pericellular matrix. *Anat Rec* **278A**, 505–513.